Changing the Transition State for Protein (Un)folding†

Donald F. Doyle,‡ Jennifer C. Waldner, Sudip Parikh, Luis Alcazar-Roman, and Gary J. Pielak*

Department of Chemistry, University of North Carolina, Chapel Hill, North Carolina 27599

Received February 20, 1996; Revised Manuscript Received April 10, 1996⊗

ABSTRACT: (Un)folding transition states of *Saccharomyces cerevisiae* iso-1-ferri- and ferrocytochromes *c* were studied using equilibrium and kinetic denaturation experiments. The wild-type protein and the global suppressor variant, N52I (isoleucine replaces asparagine 52), were examined. Denaturation was induced by guanidinium chloride (GdmCl) and monitored by circular dichroism (CD) spectropolarimetry without stopped-flow devices. Soret CD spectra indicate that thermal and GdmCl denatured states are different, and heat is the more effective denaturant. Equilibrium data show that the high stability of ferrocytochrome *c* can be rationalized as a requirement to bury the oxidation-induced positive charge and remain folded under physiological conditions. Kinetic data are monoexponential and permit characterization of the rate-limiting transition state for unfolding as a function of [GdmCl]. For the oxidized wild-type protein, the transition state solvent accessibility is nearly the same as that of the denatured state. Three perturbations, reducing the wild-type protein, reducing the N52I variant, and substituting position 52 in the oxidized protein, change the free energy and solvent accessibility of the transition state. In contrast, substituting position 52 in the reduced protein apparently does not change the transition state solvent accessibility, allowing more detailed characterization. In the reduced proteins' transition states at 4.3 M GdmCl, the position 52 side chain is in a denatured environment, even though transition state solvent accessibility is only one-third that of the denatured state (relative to the native state).

Anfinsen (1973), Merrifield (Gutte & Merrifield, 1969), and co-workers showed that a protein's amino acid sequence determines its three-dimensional structure, stability, and function. Levinthal (1968) reasoned that a path exists for the folding of the denatured protein into its native, functional state. Since these landmark reports, there has been much interest in elucidating the folding paths. Many studies focus on ferricytochromes *c*, with particular interest paid to characterizing transient intermediates. Intermediates, however, may or may not be on the path. In contrast, the transition state is guaranteed to be on the path. The de facto instability of the transition state makes it impossible to study directly, but inferences can be made by comparing the effects of perturbations on the equilibrium thermodynamics and kinetics of folding and denaturation. The principle of microscopic reversibility states that the transition state is the same for folding and unfolding.

Saccharomyces cerevisiae iso-1-cytochrome *c* contains 108 amino acid residues and a heme covalently linked via two thioethers. During the course of its function, the iron cycles between the ferri (Fe^{3+}) and ferro (Fe^{2+}) states. Several features of this protein make it desirable for structure/function studies. First, many studies of iso-1-ferricytochrome *c* stability toward guanidinium chloride (GdmCl)[1] denaturation have been reported. Second, GdmCl denaturation studies on the ferro form have been conducted indirectly using electrochemistry (Willis et al., 1993; Komar-Panicucci et al., 1994). Third, high-resolution structures of both oxidation states are available (Louie & Brayer, 1990; Berghuis & Brayer, 1992).

The global suppressor mutation (Shortle & Lin, 1985) in which asparagine 52 is replaced by isoleucine (N52I), rescues several nonfunctional cytochrome *c* variants (Das et al., 1989; Berroteran & Hampsey, 1991). When this substitution is introduced by itself, the stability (ΔG_D) of the ferri form increases (Das et al., 1989). Chemical denaturation studies on the ferro form of the N52I variant have been conducted indirectly using electrochemistry (Willis et al., 1993; Komar-Panicucci et al., 1994). Furthermore, high-resolution structures of the N52I variant in both oxidation states are available (Berghuis et al., 1994). Structural differences between the wild-type protein and the N52I variant are minor, with the exception of the change of the side chain and the expulsion of a conserved, buried water molecule.

We report kinetic and equilibrium denaturation studies of two iso-1-cytochromes *c* in both the ferri and ferro states. Experiments are directed toward characterizing the transition state for (un)folding and complement studies of transient intermediates. Together these studies will help elucidate the folding path of cytochrome *c*.

MATERIALS AND METHODS

Nomenclature. Variants are denoted using the one-letter code (IUPAC−IUB Joint Commission on Biochemical

† Supported by NIH Grant GM42501.

* Corresponding author: Phone: (919) 966-3671. FAX: (919) 962-2388. E-mail: gary_pielak@unc.edu.

‡ Present address: Howard Hughes Medical Institute, Department of Pharmacology, University of Texas Southwestern Medical Center at Dallas.

⊗ Abstract published in *Advance ACS Abstracts,* June 1, 1996.

[1] Abbreviations: CD, circular dichroism; GdmCl, guanidinium chloride; k_f, first-order rate constant for folding; k_{obs}, observed first-order rate constant; k_u, first-order rate constant for unfolding; $N52I_{OX}$, iso-1-ferricytochrome *c* with isoleucine at position 52 and threonine at position 102; $N52I_{RED}$, iso-1-ferrocytochrome *c* with isoleucine at position 52 and threonine at position 102; wt_{OX}, iso-1-ferricytochrome *c* with threonine at position 102; wt_{RED}, iso-1-ferrocytochrome *c* with threonine at position 102; [GdmCl], GdmCl concentration; ΔC_p, heat capacity of denatured state minus that of the native state; ΔG_D, stability, free energy of denatured state minus that of the native state; Θ, ellipticity; [Θ], molar ellipticity at a particular [GdmCl].

S0006-2960(96)00409-6 CCC: $12.00

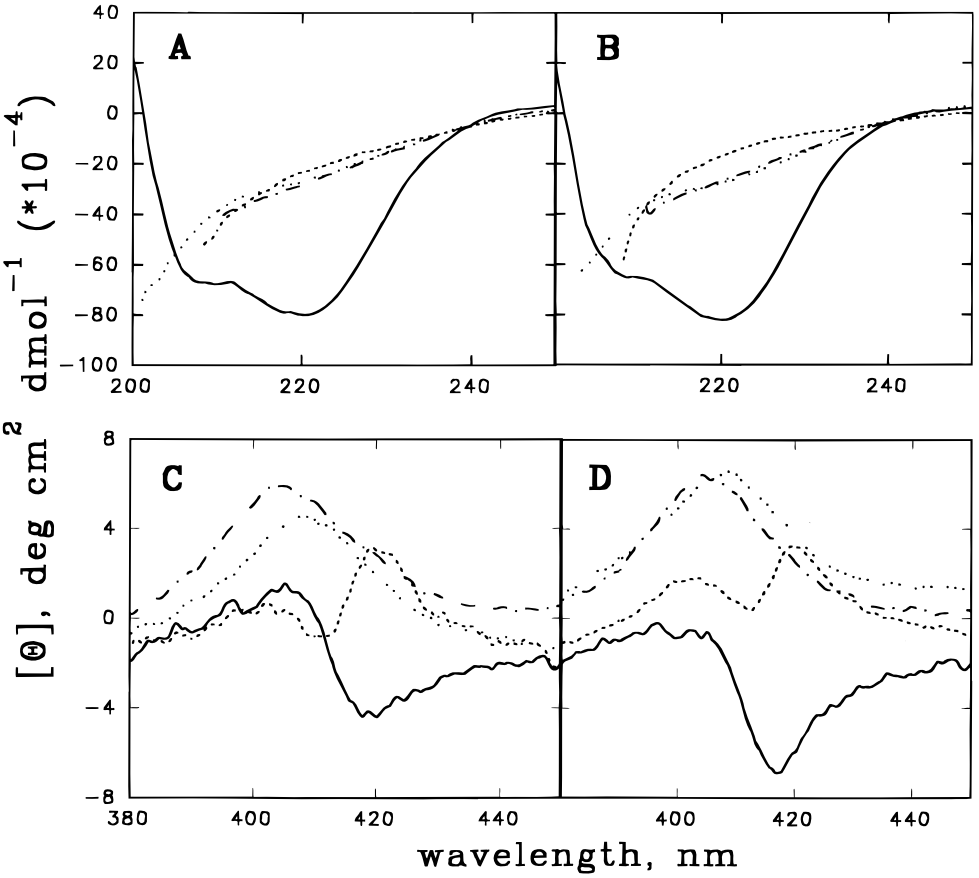

FIGURE 1: CD spectra of ferricytochrome *c* at pH 4.6, 50 mM acetate, in the far-UV (A and B) and Soret (C and D) regions: (—), native; (···), heat-denatured; (- - -), GdmCl-denatured; (- · -), GdmCl-plus-heat denatured. (A) wt_{OX}; (B) $N52I_{OX}$; (C) wt_{OX}; (D) $N52I_{OX}$.

Nomenclature, 1983) with the wild-type residue listed first, followed by the position in the amino acid sequence using the vertebrate numbering system (Moore & Pettigrew, 1990), and the variant residue. Heme oxidation states are denoted by the subscripts RED and OX, indicating ferro and ferri states, respectively. The C102T variant (Cutler et al., 1987) is used as the wild-type (wt) protein because elimination of the sole free sulfhydryl makes the protein more amenable to biophysical studies but does not change its structure or function (Berghuis & Brayer, 1992; Gao et al., 1991). The N52I variant also contains the C102T mutation.

Chemicals. GdmCl and 3-(*N*-morpholino)propanesulfonic acid (MOPS) were purchased from Sigma Chemical Company (St. Louis, MO) and used without further purification. GdmCl was dissolved in buffer, and the pH was adjusted with HCl. Stock solution concentrations varied from 5.0 to 8.0 M as evaluated by refractive index measurements (Pace et al., 1990) versus buffer at 298 K.

Proteins. Iso-1-cytochromes *c* were expressed in *S. cerevisiae*, purified using an FPLC-modified version of the method described by Willie et al. (1993), lyophilized, and stored at −70 °C. The proteins produced a single band on SDS−PAGE.

CD Spectra. Spectra were recorded in 0.100 cm path length jacketed cells on a Jasco J-600 spectropolarimeter with 1.0 nm bandwidth, automatic slit width, 0.2 nm step resolution, and a scan speed of 50 nm min^{-1}. Each point is the average of three scans, base line corrected with a buffer spectrum. Protein concentration was 30−40 μM in 50 mM sodium acetate, pH 4.6. Native state and GdmCl-denatured state spectra were acquired at 300 K. Temperatures for the heat- and GdmCl-plus-heat-denatured spectra were chosen so that the proteins were 99% denatured: 338 K for wt_{OX} and 349 K for $N52I_{OX}$. Temperature was kept within 0.2 K by a circulating water bath. For the GdmCl-denatured spectra, GdmCl concentrations were chosen at 99% denatured: 2.30 M for wt_{OX} and 3.60 M for $N52I_{OX}$. Samples were equilibrated for 10−30 min prior to data acquisition.

Far-UV and Soret CD spectra of wt_{OX} and $N52I_{OX}$ are shown in Figure 1. The pH used for these experiments was 4.6 rather than 7.0, where the kinetic and equilibrium experiments were performed, because at pH 7.0 thermal denaturation is not reversible (Betz, 1993).

Kinetics. CD experiments were performed using an Aviv CD62DS spectropolarimeter equipped with a Peltier effect thermoelectric temperature controller run in kinetics mode under N_2(g). Denaturation as a function of time at various GdmCl concentrations was monitored in the Soret region. Wavelengths of 415 nm ($C102T_{ox}$), 414 nm ($N52I_{ox}$), and 417 nm ($C102T_{red}$, $N52I_{red}$) were chosen because they exhibit the largest denaturation-induced ellipticity (Θ) change. Measurements were made using a 0.5 s time constant, 4 nm bandwidth, 1.00 cm path length, and a 0.5 s interval. Temperature was maintained at 298 K. Protein concentration was determined in 0 M GdmCl with a Shimadzu UV-160 spectrophotometer using an extinction coefficient of 106 100 M^{-1} cm^{-1} at 410 nm for oxidized proteins and 129 100 M^{-1} cm^{-1} at 416 nm for reduced proteins (Margoliash & Frohwirt, 1959). Final protein concentration was 6−10 μM in 50 mM MOPS, pH 7.0. To maintain the Fe(II) state, experiments were performed in excess $Na_2S_2O_4$.

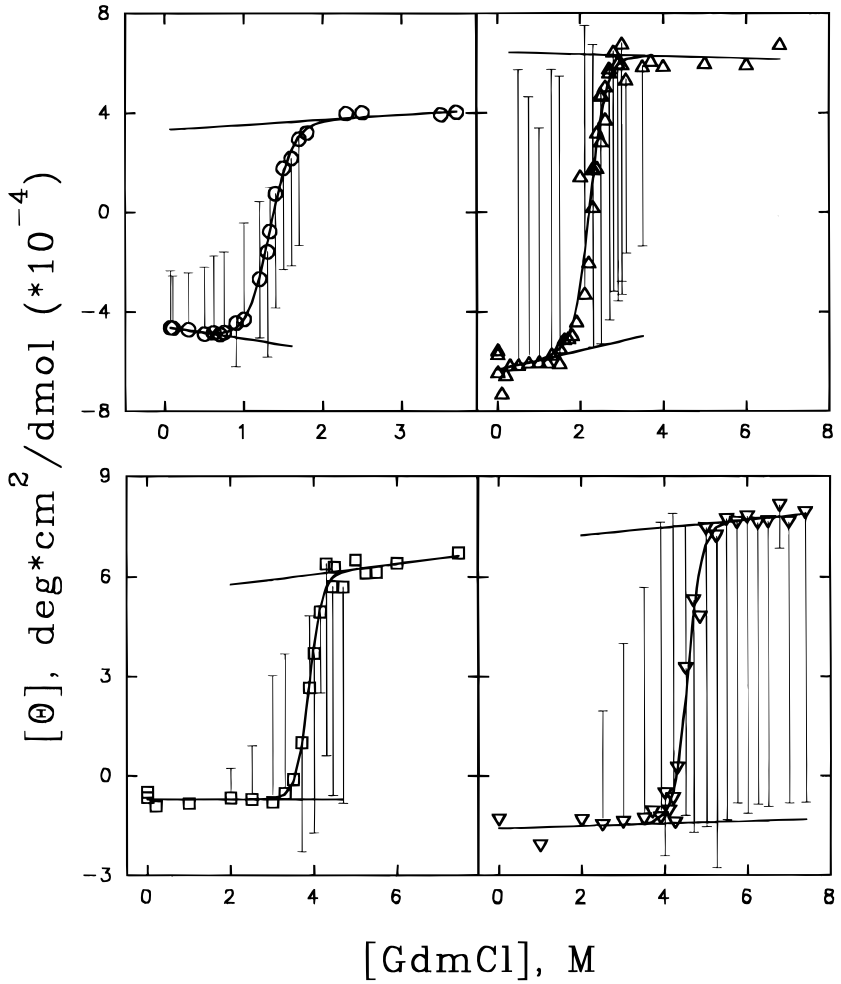

FIGURE 2: Equilibrium denaturation results: (○), wt_{OX}; (△) $N52I_{OX}$ (□) wt_{RED}; (▽), $N52I_{RED}$. The curves are the fits to eq 2. Native and denatured base lines resulting from the fit are also shown. Vertical bars indicate the amplitude for each kinetic experiment (see Kinetics under Results).

Denaturation experiments were performed by diluting stock protein solutions into various concentrations of buffered GdmCl. Dilutions were ~100 μL to 3 mL to minimize dilution-induced temperature changes. Renaturation experiments were performed by equilibrating a ~270 μM protein solution at a GdmCl concentration ([GdmCl]) corresponding to 95% denatured for as long as it took the corresponding denaturation experiment to reach equilibrium. Aliquots (100 μL) were then diluted into various concentrations of buffered GdmCl, and the return to equilibrium was monitored.

Data acquisition was initiated when the protein solution was added to the cuvette containing the GdmCl solution. The dead time was 1−3 s with a stir bar facilitating mixing. Oxidized variants require ~5 min to reach equilibrium. Reduced variants require ~10−12 min. Measurements after reaching equilibrium indicate that the pH remains 7.0 ± 0.1. We observe the slow ellipticity loss reported by Bowler et al. (1993), apparently due to aggregation of the denatured protein.

Data Analysis. Data from all kinetic experiments are well fit by the equation

$$\Theta(t) = a + b e^{-k_{obs}t} \quad (1)$$

where $\Theta(t)$ is the ellipticity at time t, a is the horizontal asymptote, b is magnitude of the difference in signal between the y-intercept and a, and k_{obs} is the observed first-order rate constant. Data were fit using a nonlinear least-squares approach.

The parameter a in eq 1, when corrected for protein concentration and path length, is the equilibrium value of the molar ellipticity ([Θ]). These values, plus equilibrium values for which kinetics could not be measured, are plotted in Figure 2. Data were fit using a nonlinear least squares approach utilizing the two-state denaturation model assuming linear base lines (Santoro & Bolen, 1988):

$$[\Theta] = \frac{m_n[\mathrm{GdmCl}] + b_n + (m_d[\mathrm{GdmCl}] + b_d)e^{-m([\mathrm{GdmCl}] - C_m)/RT}}{1 + e^{-m([\mathrm{GdmCl}] - C_m)/RT}} \quad (2)$$

where [Θ] is the molar ellipticity at a particular [GdmCl], m_n and b_n are the slope and intercept of the native state base line, m_d and b_d are the slope and intercept of the denatured state base line, C_m is the [GdmCl] at the transition midpoint, m is the slope of a ΔG_D versus [GdmCl] plot, and RT is the product of the gas constant and the absolute temperature. The denaturation free energy in the absence of denaturant, $\Delta G_{D,H2O}$, is the intercept of the ΔG_D versus [GdmCl] plot.

Kinetic data at all [GdmCl] are summarized in Figure 3. For a reversible two-state reaction, k_{obs} is the sum of the

Table 1: Equilibrium and Kinetic Parameters[a]

method	$m_f^{\ddagger}$ [b]	$b_f^{\ddagger}$ [c]	$m_f^{\ddagger}$ [b]	$b_f^{\ddagger}$ [c]	m[b]	C_m[d]
wt_{OX}						
1[e]	nc[h]	nc	-3.8 ± 0.2	6.9 ± 0.3	-4.2 ± 0.5	1.33 ± 0.02
2[f]	0.3 ± 0.2	1.49 ± 0.07	na[i]	na	na	na
3[g]	1.1 ± 0.4	1.0 ± 0.5	-3.0 ± 0.5	5.6 ± 0.6	-4.1 ± 0.6	1.10 ± 0.07
$N52I_{OX}$						
1	nc	nc	-1.7 ± 0.1	6.5 ± 0.3	-3.0 ± 0.6	2.25 ± 0.05
2	1.2 ± 0.1	0.2 ± 0.3	-0.8 ± 0.1	3.5 ± 0.4	-2.0 ± 0.1	1.6 ± 0.2
3	1.3 ± 0.1	0.1 ± 0.3	-1.9 ± 0.2	7.0 ± 0.4	-3.2 ± 0.2	2.14 ± 0.07
wt_{RED}						
1	nc	nc	-1.5 ± 0.2	8.1 ± 0.7	-3.8 ± 0.5	3.88 ± 0.03
2	0.25 ± 0.01	1.22 ± 0.03	-1.1 ± 0.8	6.2 ± 3.8	-1.3 ± 0.8	3.9 ± 0.5
3	0.4 ± 0.3	0.9 ± 1.3	-1.3 ± 0.4	7.5 ± 1.6	-1.7 ± 0.5	3.9 ± 0.4
$N52I_{RED}$						
1	nc	nc	-1.30 ± 0.07	9.8 ± 0.4	-3.9 ± 0.8	4.53 ± 0.04
2	1.0 ± 0.1	-1.0 ± 0.3	-1.15 ± 0.09	8.9 ± 0.6	-2.2 ± 0.1	4.6 ± 0.1
3	1.18 ± 0.06	-1.7 ± 0.3	-1.47 ± 0.08	10.7 ± 0.4	-2.7 ± 0.1	4.70 ± 0.05

[a] Uncertainties are one standard deviation of the fit to the approprite equation, or one standard deviation of the fit to the appropriate equation followed by propagation of error analysis. To obtain accurate uncertainties, modified forms of the equations were used where [GdmCl] was replaced by ([GdmCl] − $[GdmCl]_{average}$). [b] kcal mol^{-1} M^{-1}. [c] kcal mol^{-1}. [d] M. [e] Uses dependent k_u and K_D. [f] Uses k_u and k_f outside transition region. [g] Deconvolutes k_{obs} into k_u and k_f. [h] nc, not calculated. [i] na, not available.

first-order rate constant for unfolding, k_u, and the first-order rate constant for folding, k_f (Matouschek et al., 1990).

$$k_{obs} = k_u + k_f \tag{3}$$

Plots of $-RT \ln(k_u)$ and $-RT \ln(k_f)$ versus [GdmCl] are frequently linear (Tanford, 1970). The slopes and intercepts of these plots are $m_u^{\ddagger}$ and $b_u^{\ddagger}$ and $m_f^{\ddagger}$ and $b_f^{\ddagger}$, respectively.

$$-RT \ln(k_u) = m_u^{\ddagger}[GdmCl] + b_u^{\ddagger} \tag{4}$$

$$-RT \ln(k_f) = m_f^{\ddagger}[GdmCl] + b_f^{\ddagger} \tag{5}$$

Thus, k_{obs} versus [GdmCl] plots are described by four kinetic parameters, $m_u^{\ddagger}$, $b_u^{\ddagger}$, $m_f^{\ddagger}$, and $b_f^{\ddagger}$. These kinetic parameters can be used to calculate the *equivalent* of the equilibrium parameters C_m and m:

$$C_m = \frac{b_u^{\ddagger} - b_f^{\ddagger}}{m_f^{\ddagger} - m_u^{\ddagger}} \tag{6}$$

$$m = m_u^{\ddagger} - m_f^{\ddagger} \tag{7}$$

RESULTS

wt_{OX} and $N52I_{OX}$ CD spectra. The native states of wt_{OX} and $N52I_{OX}$ are indistinguishable in the far-UV (Figure 1). This observation is consistent with the fact that the fold of both proteins is the same (Berghuis et al., 1994). The far-UV spectra are also identical in the heat- and GdmCl-plus-heat-denatured states. In contrast, wt_{OX} has a consistently more negative ellipticity in the GdmCl-denatured state than does $N52I_{OX}$. Neither denatured state has a random coil spectrum (Brahms & Brahms, 1980), suggesting residual structure. Bowler et al. (1994) also report residual structure in the GdmCl-denatured state of the oxidized C102S variant.

The Soret region is a sensitive probe of the environment on the Met-80 side of the heme (Pielak et al., 1986). In this region only the GdmCl-plus-heat-denatured state spectra are clearly the same for the two proteins (Figure 1). Comparison of the native state spectra shows that the negative Soret Cotton effect is larger in the $N52I_{OX}$ protein. Comparison of the GdmCl-denatured state spectra shows that the ∼400 nm positive Cotton effect of $N52I_{OX}$ is nearly absent in the wt_{OX} spectrum while the ∼420 nm positive Cotton effects are almost identical. Comparison of the heat-denatured state spectra shows that the profiles are the same, but the ellipticities of $N52I_{OX}$ are uniformly more positive. Although this discrepancy may reflect structural differences, it may also be due to the temperature difference.

Equilibrium Thermodynamic Parameters from End Kinetics. Equilibrium GdmCl denaturation of yeast cytochromes *c* and many variants is reversible and complete in 5 min (Ramdas & Nall, 1986; Nall, 1983; Bowler et al., 1993; Hickey et al., 1991). In our studies, renaturation equilibrium ellipticities lie on the native base line. Therefore, within the time of these experiments (<30 min), denaturation is reversible for all four proteins.

The reduced proteins are oxidized by atmospheric oxygen, and the denatured state is oxidized faster than the native state. Nevertheless, the ferro proteins remain reduced over the course of the experiments as determined by an insignificant change in absorbance at 550 nm upon addition of $Na_2S_2O_4$ after equilibrium was reached. Therefore, under the conditions of these experiments, unfolding is fast relative to oxidation but slow enough to be monitored without stopped-flow devices.

Equilibrium data for all proteins are well fit by a two-state model (Figure 2). Two further observations provide additional evidence for two-state behavior: (1) the kinetic data are well represented by a single exponential, and (2) the use of kinetic *a* values (eq 1) as equilibrium values gives parameters that agree with classically obtained equilibrium parameters (vide infra). The measured equilibrium parameters m and C_m are presented in Table 1 (method 1), and $\Delta G_{D,H2O}$ values are presented in Table 2.

Hickey et al. (1991) report thermal and chemical denaturation ΔG_D values for similar cytochrome *c* variants that are in reasonable agreement. Given the difference in denatured states (Figure 1), however, we restrict comparisons to GdmCl denaturation studies.

The $\Delta G_{D,H2O}$ value for wt_{OX} agrees with values for similar variants obtained between pH 7.0 and 7.5 [4.7 ± 0.5 kcal mol^{-1} (Hickey et al., 1991); 6.4 ± 0.3 kcal mol^{-1} (Betz &

Table 2: Derived Parameters

protein	$\Delta G_{D,H2O}$ [a]	$m_u^{\ddagger}/m$ [b]
wt_{OX}	5.6 ± 0.8	0.9 ± 0.1
$N52I_{OX}$	6.8 ± 1.4	0.6 ± 0.1
		0.47 ± 0.05[c]
wt_{RED}	15 ± 2	0.40 ± 0.07
$N52I_{RED}$	18 ± 4	0.33 ± 0.07

[a] $\Delta G_{D,H20} = mC_m$. Units are in kcal mol^{-1}. The uncertainty is from the standard deviation of the fit to eq 2 and propagation of error analysis. [b] $m_u^{\ddagger}$ from method 1. [c] Relative to authentic equilibrium data (see text).

Pielak, 1992); 6.3 ± 0.3 kcal mol^{-1} (Auld, 1993); 5.6 ± 0.4 kcal mol^{-1} (Bowler et al., 1993); 6.6 ± 0.3 kcal mol^{-1} (Hilgen-Willis, 1993); 5.0 ± 0.5 kcal mol^{-1} (Komar-Panicucci et al., 1994); 5.9 ± 0.3 kcal mol^{-1} (Linske-O'Connell et al., 1995)]. Another value is significantly lower [1.57 kcal mol^{-1} (Koshy et al., 1994)], probably because Koshy et al. used the true wild-type protein.

The $-m$ value for wt_{OX} agrees with values for similar variants obtained between pH 7.0 and 7.5 [3.9 ± 0.5 kcal mol^{-1} M^{-1} (Hickey et al., 1991); 4.6 ± 0.2 kcal mol^{-1} M^{-1} (Betz & Pielak, 1992); 4.2 ± 0.3 kcal mol^{-1} M^{-1} (Auld, 1993); 4.9 ± 0.3 kcal mol^{-1} M^{-1} (Bowler et al., 1993); 4.6 ± 0.2 kcal mol^{-1} M^{-1} (Hilgen-Willis, 1993); 3.9 ± 0.2 kcal mol^{-1} M^{-1} (Komar-Panicucci et al., 1994); 4.4 kcal mol^{-1} M^{-1} (Linske-O'Connell et al., 1995)]. Another value is significantly lower [0.91 kcal mol^{-1} M^{-1} (Koshy et al., 1994)].

For $N52I_{OX}$, $\Delta G_{D,H2O}$ is within the uncertainty of a similar variant (N52I;C102A) between pH 7.0 and 7.2 [7.0 ± 0.5 kcal mol^{-1} (Hickey et al., 1991)]. Our value, however, is significantly smaller than those from two other reports [9.0 ± 0.5 kcal mol^{-1} (Komar-Panicucci et al., 1994); 10.0 ± 0.5 kcal mol^{-1} (Linske-O'Connell et al., 1995)] and significantly larger than that of Koshy et al. (1994; 3.02 kcal mol^{-1}). Despite these differences, Koshy et al. (1994) report a similar stability increase upon changing asparagine 52 to isoleucine (1.5 kcal mol^{-1}).

Because the $N52I_{OX}$ end-kinetic data give a smaller stability increase than other reports, a conventional equilibrium denaturation was performed. All measurements were performed on the same day with a 20−30 min equilibration time. The resulting parameters (C_m = 2.22 ± 0.02 M, m = 3.6 ± 0.3 kcal mol^{-1} M^{-1}, $\Delta G_{D,H2O}$ = 8.0 ± 0.7 kcal mol^{-1}) are within uncertainty of the end-kinetic results (Table 1, method 1) but bring the stability increase closer to earlier measurements. This result gives us confidence in the end-kinetic values.

For $N52I_{OX}$, $-m$ is within the uncertainty of a similar variant (N52I;C102A) between pH 7.0 and 7.2 [3.6 ± 0.5 kcal mol^{-1} M^{-1} (Hickey et al., 1991)]. Our value, however, is significantly smaller than two reports [4.2 ± 0.2 kcal mol^{-1} (Komar-Panicucci et al., 1994)]; 4.77 kcal mol^{-1} (Linske-O'Connell et al., 1995)] and significantly larger than that of Koshy et al. (1994; 1.39 kcal mol^{-1}).

The increased $\Delta G_{D,H2O}$ upon reduction of the wild-type protein calculated from the data in Table 2 (9.4 ± 2.2 kcal mol^{-1}) matches the value for GdmCl denaturation at pH 4.6 from electrochemistry [10.1 ± 0.4 kcal mol^{-1} (Hilgen-Willis et al., 1993)] and for a closely related variant, C102A [10.7 ± 0.3 kcal mol^{-1} (Komar-Panicucci et al., 1994)]. Thus, the stability increase is pH insensitive. The uncertainty in

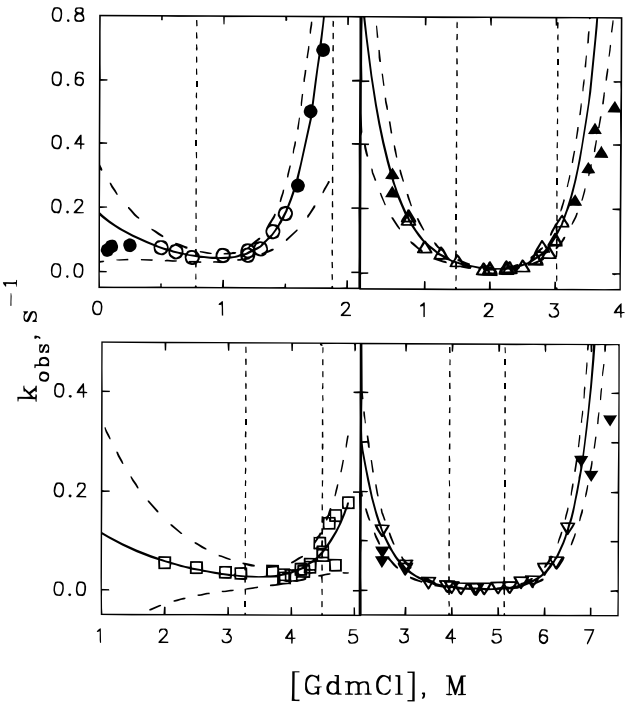

FIGURE 3: Plots of k_{obs} versus [GdmCl]. Symbols are from the legend to Figure 2. Open symbols are data used in the method 3 fit to eq 8. Solid curves are the result of the fit. Dashed curves are the fit curve ± one standard deviation. Vertical bars indicate [GdmCl] at which the protein is 98% native and 98% denatured.

$\Delta G_{D,H2O}$ for the reduced proteins is larger than that for the oxidized proteins because extrapolation to 0 M GdmCl is longer. The extrapolation is justified because the directly measured stabilities agree with those from electrochemistry.

The increase in $\Delta G_{D,H2O}$ upon reduction of the N52I protein (11.2 ± 4.2 kcal mol^{-1}, Table 2) agrees with that calculated from the electrochemical method at pH 4.6 for both this protein [9.4 ± 0.4 kcal mol^{-1} (Willis et al., 1993)] and a closely related variant, N52I;C102A [9.4 ± 0.3 kcal mol^{-1} (Komar-Panicucci et al., 1994)].

Kinetics. In Figure 2 the vertical bars depict amplitudes, the *observed* ellipticity range in a kinetic experiment. The limit of each bar is the molar ellipticity of the first point used in the exponential fit (eq 1), and the symbol represents the equilibrium value (a in eq 1). If 100% of the folding (unfolding) amplitude is observed, the vertical bar extends from the extrapolated denatured (native) base line to the symbol. For clarity, amplitudes are not shown for all experiments. Anomalously small amplitudes are due to occasional instrument or operator error leading to longer dead times. Nevertheless, rate constants from these experiments follow the same trends as rate constants from data collected over a larger ellipticity range (Figure 4). Values of k_{obs} range from 0.002 to 0.75 s^{-1}.

The transition state explored here appears to correspond to the slowest unfolding phase of iso-2-cytochrome *c* [k_{obs} = $1/\tau$ = 0.01−0.05 s^{-1} (Nall & Landers, 1981)] and the slow but minor phase of equine cytochrome *c* unfolding [k_{obs}= $1/\tau$ = 0.3 s^{-1}, (Ridge et al., 1981)]. In terms of folding, this transition state corresponds to the Soret-absorbance detected slow phases of iso-2- and equine cytochromes *c* (Osterhout & Nall, 1985; Elöve et al., 1994). In those reports, however, this slow phase accounts for only 30% of the amplitude in iso-2-cytochrome *c* folding and is not observed by fluorescence.

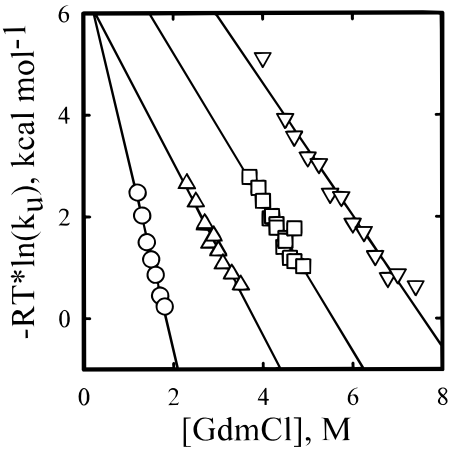

FIGURE 4: Plot of $-RT\ln(k_u)$ (method 1) versus [GdmCl]. Symbols are from the legend to Figure 2.

In contrast to reports on other cytochromes *c*, we observe monoexponential kinetics that account for ~100% of the signal change between the native and denatured states. The discrepancies arise because of our longer dead time (obviating detection of early intermediates) and the fact that, at the wavelengths used, CD is sensitive primarily to the environment on the Met-80 side of the heme (Pielak et al., 1986).

At C_m, k_{obs} for folding equals k_{obs} for unfolding for all four proteins. This observation proves that the unfolding kinetics do not correspond to dissociation of polymeric protein produced by lyophilization (Nall & Landers, 1981).

To determine the effect of ionic strength, a kinetic experiment was performed on each protein at its C_m and an ionic strength of 24 M^2 (i.e., [GdmCl] + [NaCl] = 4.9 M). Neither k_{obs} nor *a* is strongly ionic strength dependent.

DISCUSSION

Heat and GdmCl Produce Different Denatured States. For each protein the GdmCl-denatured state is different from the heat-denatured state (Figure 1). This effect is particularly striking in the Soret spectra. When both GdmCl and heat are used, the spectra are very similar to those from heat denaturation alone, indicating that heat is the more effective denaturant. The difference in denatured state structures may account for the discrepancy in stability upon reduction at pH 4.6 and 300 K between thermal denaturation [6.6 ± 0.8 kcal mol^{-1} (Cohen & Pielak, 1995)] and GdmCl denaturation determined electrochemically [10.1 ± 0.4 kcal mol^{-1} (Hilgen-Willis et al., 1993)]. Paradoxically, although heat is the more effective denaturant, stability is actually greater toward GdmCl. In summary, for each oxidized protein, thermal and GdmCl denatured states are different, and heat is the more effective denaturant.

Equilibrium Data. Our equilibrium results agree with other reported values (see Results). Both the $N52I_{OX}$ and $N52I_{RED}$ variants are more stable than their wild-type counterparts.

Values of *m* (eq 2) and ΔC_p, the heat capacity of the denatured state minus that of the native state, are interpreted in terms of differences in solvent-exposed surface area between the native and denatured states (Schellman, 1978; Shortle & Meeker, 1986; Murphy et al., 1992; Spolar et al., 1992; Myers et al., 1995). Neither mutagenesis nor reduction changes either *m* (Table 1, method 1) or ΔC_p (Cohen & Pielak, 1995; D. F. Doyle, unpublished observations). This observation is at first surprising because both perturbations change the hydrophobicity of the solvent-exposed denatured state, which should affect *m* and ΔC_p. The fact that *m* is refractory, however, is in accord with the idea that the heme remains ligated in the denatured state near neutral pH (Muthukrishnan & Nall, 1991) and renders the changes in $m_u^{\ddagger}$ even more remarkable.

Kinetics. The kinetics of GdmCl-induced denaturation is well fit by a single exponential and is ionic strength independent. The transition states probed here correspond to the overall rate-limiting step of denaturation because we observe the slowest unfolding phase. From the Eyring equation, the activation free energy is obtained by adding a constant (17.6 kcal mol^{-1} at 300 K) to $b_u^{\ddagger}$. Changes in activation free energy are equal to differences in $b_u^{\ddagger}$. This approach avoids the potential complications of applying traditional transition state theory, which is based on covalent bond making/breaking, to a transition state that may not involve making or breaking covalent bonds. Although this approach *is* based on transition state theory

$$k_u = pe^{-\Delta G_u^{\ddagger}/RT} \tag{8}$$

the approach is *not* based on any particular form of the theory (Fersht et al., 1992). Traditionally, *p* in eq 8 is k_BT/h, where k_B is Boltzmann's constant and *h* is Planck's constant. By assuming *p* is 1 s^{-1}, eq 4 can be defined (physically unrealistically) as the unfolding activation free energy. This assumption avoids the inappropriate use of traditional transition state theory. Here, only changes in activation free energies (differences in $b_u^{\ddagger}$ values) are important.

We evaluated the kinetic data using three methods and the resulting parameters are given in Table 1. In method 1, equilibrium thermodynamic parameters are combined with kinetic *denaturation* data to obtain the kinetic parameters. Only the denaturation parameters ($m_u^{\ddagger}$, $b_u^{\ddagger}$) are calculated because of the existence of folding intermediates (vide infra). At any [GdmCl], the equilibrium constant for denaturation, K_D, is calculated from equilibrium data. Using the relationship $k_{obs} = k_u(1 + 1/K_D)$, k_u is obtained from k_{obs} and K_D. Plots of $-RT\ln(k_u)$ versus [GdmCl] are shown in Figure 4. Linear fits of the data in Figure 4 have a reduced $\chi^2 \approx 1$, therefore, higher order fits are not justified.

In method 2, kinetic data are evaluated nearly independently of equilibrium data. Equilibrium thermodynamic data are used to determine the transition region, the [GdmCl] range at which the protein is between 98% native and 98% denatured (vertical lines in Figure 3). At [GdmCl] below or above this region, k_{obs} is determined solely by k_f or k_u, respectively. Plots of $-RT\ln(k_{obs})$ versus [GdmCl] were made for each high and low [GdmCl] range, and linear regression was used to obtain $m_u^{\ddagger}$, $b_u^{\ddagger}$, $m_f^{\ddagger}$, and $b_f^{\ddagger}$.

In method 3, the kinetic data are fit to the kinetic two-state equation obtained from combining eq 3−5

$$k_{obs} = e^{\frac{-(m_u^{\ddagger}[\mathrm{GdmCl}] + b_u^{\ddagger})}{RT}} + e^{\frac{-(m_f^{\ddagger}[\mathrm{GdmCl}] + b_f^{\ddagger})}{RT}} \tag{9}$$

using a nonlinear least-squares approach. Results of the fits are the solid curves in Figure 3.

The three methods are complementary, and each method has advantages and disadvantages. Method 1 gives kinetic parameters that depend on the measured equilibrium parameters, precluding independent evaluation. This method, however, focuses on the most accurately determined parameters (m, C_m, $m_u^‡$, and $b_u^‡$) which are also the most valuable for characterizing the transition state.

Method 2 results in measured and equivalent equilibrium parameters that are nearly independent. The kinetic parameters are used to calculate equivalent equilibrium parameters which are compared to the measured ones (reported under method 1). The comparison provides an objective evaluation of the kinetic parameters. Furthermore, the two folding parameters are independent of the two unfolding parameters. There are two possible problems, however. First, the kinetic data are from outside the equilibrium transition region. Extrapolation into this region is invalid if intermediates exist. Second, in regions of [GdmCl] at which kinetic data must be collected for k_{obs} to equal k_f (or k_u), the reaction may be too fast to measure.

In method 3, kinetic data are evaluated independently of measured equilibrium thermodynamic parameters. Like method 2, equivalent equilibrium parameters can be calculated to objectively evaluate the kinetic parameters. Unlike method 2, the limitation of extrapolating to the transition region does not apply because the data are from the transition region. Furthermore, the method 2 limitation of collecting kinetic data in regions where the reaction is too fast is less stringent. Indeed, method 3 allows determination of unfolding kinetic parameters for wt_{OX} that could not be obtained using method 2. Unlike method 2, however, the folding parameters are not independent of the unfolding parameters. Therefore, complications from folding intermediates may affect the unfolding parameters. This limitation is partially ameliorated by excluding kinetic data at [GdmCl] where an intermediate is observed. This is done for wt_{OX} by eliminating the kinetic values at the three lowest [GdmCl] from the fit. Additionally, the other methods require transformation of kinetic data to free energy space (where units are kcal mol^{-1}) before the kinetic parameters can be calculated. In method 3, kinetic data are fit directly.

In general, methods 2 and 3 are used to evaluate $m_u^‡$ and $b_u^‡$ obtained by method 1. The method 1 values are then used to make inferences about the transition state. Insights gained from methods 2 and 3 are also used to make inferences about the populated states on either side of the transition state (i.e., native state, denatured state, or an intermediate).

The classic evidence for folding intermediates is the observation of folding rate constants (usually at low [GdmCl]) smaller than expected from two-state kinetics (Matouschek et al., 1990). Although less common than folding intermediates, unfolding intermediates have been observed (Kiefhaber et al., 1995). Using kinetic data from [GdmCl] where intermediates are observed to extrapolate into the transition region is inappropriate and causes a discrepancy between the measured and equivalent equilibrium parameters. Additionally, intermediates may be deduced from a discrepancy between measured and equivalent equilibrium parameters when other reasons for the discrepancy have been ruled out.

Amplitudes are also useful for detecting intermediates. Amplitudes may be less than the expected signal change for two reasons. First, a fast forming intermediate may be present that has a different response to the probe than the native or denatured states. Second, the reaction may be so fast that significant signal loss occurs in the dead time. With a 3 s dead time, if $k_{obs} \leq 0.2\ s^{-1}$ and the reaction is two-state, then the amplitude will be more than half of the expected signal change. Therefore, only kinetic data with $k_{obs} \leq 0.2\ s^{-1}$ are used in method 3 to increase confidence in the identification of intermediates.

For wt_{OX}, $m_u^‡$ and $b_u^‡$ cannot be calculated by method 2 because unfolding is too fast for us to measure where $k_{obs} = k_u$ ([GdmCl] $\geq$ 1.88 M). Note the absence of data in Figure 3 at [GdmCl] where the protein is $\geq$98% denatured. There is a folding intermediate at low [GdmCl] because k_{obs} is lower than expected and because the amplitudes are small even though $k_{obs} \leq 0.2\ s^{-1}$. This observation means that k_f has contributions from at least two states and renders $m_f^‡$ and $b_f^‡$ values from method 2 useless. To minimize the effect of the folding intermediate on method 3, k_{obs} at the three lowest [GdmCl] were not included in the fit. The agreement between the measured and equivalent equilibrium parameters is remarkable considering that some effect of the intermediate is present. Because the influence of the intermediate is propagated by method 3, and because the three k_{obs} values $>0.2\ s^{-1}$ fall very close to the fit line, it is concluded that $m_u^‡$ and $b_u^‡$ from method 1 for wt_{OX} are valid and describe the transition between the native state and the transition state.

For $N52I_{OX}$, the equivalent equilibrium parameters from method 2 do not agree with the measured values (method 1). The reason for the disparity becomes clear by examining the method 3 fit (Figure 3), for which the equivalent equilibrium parameters agree with the measured ones. Contrary to the observation for wt_{OX}, k_{obs} values $> 0.2\ s^{-1}$ are not close to the fit line. Thus, either the reaction is too fast for us to measure reliably or there is an unfolding intermediate. Under these circumstances it is inappropriate to use $m_u^‡$ and $b_u^‡$ values from method 2. Values of $m_f^‡$ and $b_f^‡$ from methods 2 and 3 agree; therefore, there is no evidence for a folding intermediate. The $m_u^‡$ and $b_u^‡$ values from method 1 are valid because $m_u^‡$, $b_u^‡$, m, and C_m values from methods 1 and 3 are within the uncertainty of each other. These parameters, however, describe the transition between either the native state or an intermediate and the transition state. Lacking compelling evidence for an unfolding intermediate, we interpret the parameters as describing the transition between the native state and the transition state for $N52I_{OX}$.

For wt_{RED}, the equivalent C_m from methods 2 and 3 are in good agreement with the measured C_m. Given the disagreement between the equivalent m values and the measured m value, however, the agreement is not meaningful. Although the kinetic folding parameters from methods 2 and 3 are within uncertainty of each other, and no classical evidence for a folding intermediate is seen (Figure 3), a folding intermediate is still present because anomolously small amplitudes are observed at low [GdmCl] (Figure 2). The kinetic unfolding parameters from all three methods agree. Therefore, the $m_u^‡$ and $b_u^‡$ values from method 1 for wt_{RED} are valid and describe the transition between the native state and the transition state. For $N52I_{RED}$, the conclusions are identical to those for wt_{RED}.

In summary, for all four proteins $m_u^{\ddagger}$ and $b_u^{\ddagger}$ from method 1 describe the transition between the native state and the rate-limiting transition state. There is evidence of a folding intermediate for wt_{OX}, wt_{RED}, and $N52I_{RED}$ but not for $N52I_{OX}$. There may be an unfolding intermediate for $N52I_{OX}$, but there is no evidence of an unfolding intermediate for wt_{OX}, wt_{RED}, and $N52I_{RED}$.

Combining Equilibrium and Kinetic Data. The ratio $m^{\ddagger}/m$ measures the increase in transition state solvent exposure from the native state relative to that in the denatured state (Tanford, 1970). For a kinetic two-state mechanism, $m_f^{\ddagger}$ or $m_u^{\ddagger}$ may be used as an indication of transition state solvent exposure. Due to the detection of folding intermediates, we use only $m_u^{\ddagger}/m$ (Table 2).

In contrast to other proteins (where $m_u^{\ddagger}/m \approx 0.3$; Matouschek & Fersht, 1993; Jackson & Fersht, 1991; Milla et al., 1995; Parker et al., 1995) the wt_{OX} transition state is nearly as solvent exposed as the denatured state (i.e., $m_u^{\ddagger}/m$ approaches unity). Analysis of the data of Ikai et al. (1973) reveals that $m_u^{\ddagger}/m$ also approaches unity for equine ferricytochrome *c* at pH 6.5. The N52I substitution dramatically reduces the solvent exposure of the transition state relative to the denatured state. For the ferro forms, $m_u^{\ddagger}/m$ is significantly smaller than for the ferri forms but not significantly different from each other. Also, $m_u^{\ddagger}/m$ for the ferro forms is similar to that for other proteins.

If $m_u^{\ddagger}/m$ changes, either the unfolding path has changed (the converse is not necessarily true) or the same sequential path is followed but the rate-determining step has changed. Kinetic experiments monitoring all transitions are required to resolve the ambiguity, but because three of the four perturbations drastically alter $m_u^{\ddagger}/m$ it is likely that the path has changed. This result is in contrast to other proteins for which substitutions have only a small effect on $m_u^{\ddagger}/m$ (Matouschek & Fersht, 1993; Matouschek et al., 1995; Milla et al., 1995). Here, the only change that *does not* significantly affect $m_u^{\ddagger}/m$ is the N52I substitution in the reduced protein. In summary, reducing the wild-type protein, reducing the N52I variant, and changing the residue at position 52 in the oxidized protein change the unfolding path, but changing the residue at position 52 in the reduced protein apparently does not.

Changes in the Native, Denatured, and Transition States. The redox-induced stability difference is expected to affect the free energy of both the native and denatured states. Upon oxidation, the net charge of the heme core (iron and nitrogens) changes from 0 to +1. Burial of this charge destabilizes the native state and stabilizes the more solvent-exposed denatured state. Both effects lead to a smaller stability for the oxidized protein. In summary, the greater stability of the reduced proteins may be necessary for the protein to bury the oxidation-induced positive charge and remain folded under physiological conditions.

Changing asparagine 52 to isoleucine increases stability. The stability increase is due to perturbation of both the native and denatured states. The hydrophobic-for-hydrophilic substitution destabilizes the denatured state without significantly affecting its solvent accessible surface area. Consistent with this idea, *m* and ΔC_p are unchanged. This substitution is expected to stabilize the native state primarily because it is accompanied by expulsion of a buried water. Both effects lead to a more stable protein with isoleucine at position 52.

Reduction and substituting isoleucine for asparagine at position 52 have various effects on the relative free energies of the native and transition states (i.e., unfolding activation free energies). The effect of the N52I substitution on $b_u^{\ddagger}$ is insignificant in the oxidized state (-0.4 ± 0.4 kcal mol^{-1}) but significant in the reduced state (1.7 ± 0.8 kcal mol^{-1}). Reduction increases $b_u^{\ddagger}$ for both the wt protein and the N52I variant.

Changes in $m_u^{\ddagger}/m$ can be due to any combination of native, transition, and denatured state effects. In this case, however, we can assign the change to the transition state because *m* does not change and the crystal structures are nearly identical (Berghuis et al., 1994).

Our data strengthen the proposal of Elöve et al. (1994) that the oxidized protein transition state corresponds to Fe−S bond breaking, because Soret CD probes the environment on the Met-80 side of the heme, and because the rate determining transition state is nearly completely solvent exposed. On the other hand, the transition state for the reduced proteins appears not to correspond to Fe−S bond breaking because $m_u^{\ddagger}/m$ values are similar to those of non-heme proteins. This conclusion is consistent with data from studies of reduced equine cytochrome *c* where "the dynamics of ligand binding and dissociation are much faster in the reduced state" (Elöve et al., 1994). In the reduced proteins, the N52I substitution increases $b^{\ddagger}$ without affecting $m_u^{\ddagger}/m$. These observations suggest that the transition state of the reduced proteins involves solvent invasion into the hydrophobic core. This idea is consistent with the fact that more energy is required to solvate the ferrous heme than the ferric heme (Cohen & Pielak, 1995, and references therein). In summary, the transition state of the oxidized proteins involves Fe−S bond breaking, and the transition state of the reduced proteins probably involves solvent invasion into the hydrophobic core. Finally, it is interesting to note that the oxidized proteins are *similar* to other proteins with respect to stability and *different* from other proteins with respect to transition state solvent exposure, but the reduced proteins follow the *opposite* trends.

Φ *Analysis.* In general, the greater the stability, the greater the activation free energy (Tables 1 and 2). However, the dramatic stability increase upon reduction (∼10 kcal mol^{-1}) is only partially reflected in increased activation free energy (∼1 to 3 kcal mol^{-1}). Structural interpretations of these free energy differences are obtained using Φ values (Matouschek et al., 1989). The Φ value is defined as $\Delta\Delta G_D^{\ddagger}/\Delta\Delta G_D$ and is determined experimentally (in the absence of denaturant) as $(b_{var}^{\ddagger} - b_{wt}^{\ddagger})/(\Delta G_{D,H2O,var} - \Delta G_{D,H2O,wt})$, where var refers to a variant protein. Interpretation of Φ uses the relation $\Phi = (\Delta G_F - \Delta G^{\ddagger})/(\Delta G_F - \Delta G_{SOLV})$, where ΔG_F is free energy difference of the native states, $\Delta G^{\ddagger}$ is the free energy difference of the transition states, and ΔG_{SOLV} is the free energy difference of the denatured states (Matouschek et al., 1989). Structural interpretations of Φ provide information about solvent exposure of the perturbed site in the transition state relative to that in the native and denatured states.

If the unfolding path is unchanged, a Φ value of one means that at the site of the perturbation the transition state is the same as the denatured state. A Φ value of zero means that at the site of the perturbation, the transition state is the same

as the native state. It may be correct to place a structural interpretation on Φ for the N52I substitution in the reduced form, because $m_u^{\ddagger}/m$ does not change (Table 2). In the absence of GdmCl, $\Phi = 0.6 \pm 0.9$, but the uncertainty obviates interpretation. The uncertainty in Φ is a minimum at 4.3 M GdmCl where $\Phi = 0.96 \pm 0.14$. Therefore, at 4.3 M GdmCl, the position 52 side chain is in the same environment in the transition state as it is in the denatured state. From $m_u^{\ddagger}/m$, the solvent accessibility of the transition state is approximately one-third that of the denatured state relative to the native state. In summary, the native state interactions of the position 52 side chain are absent in the transition state even though the transition state solvent accessibility is only 35% that of the denatured state (relative to the native state).

ACKNOWLEDGMENT

We thank Chuck Hardin for use of the Jasco J-600, Aleister Saunders for some of the wild-type protein used in this study and for assistance in operating the Jasco J-600, and members of the Pielak group for comments on the manuscript. We thank an anonymous reviewer for pointing out the dependence of the kinetic parameter $m_u^{\ddagger}$ on the equilibrium parameters in method 1.

REFERENCES

Anfinsen, C. B. (1973) *Science 181*, 223−230.
Auld, D. S. (1993) Doctoral Dissertation, University of North Carolina at Chapel Hill.
Berghuis, A. M., & Brayer, G. D. (1992) *J. Mol. Biol. 223*, 959−976.
Berghuis, A. M., Guillemette, J. G., McLendon, G., Sherman, F., Smith, M., & Brayer, G. D. (1994) *J. Mol. Biol. 236*, 786−799.
Berroteran, R. W., & Hampsey, M. (1991) *Arch. Biochem. Biophys. 288*, 261−269.
Betz, S. F. (1993) Doctoral Dissertation, University of North Carolina at Chapel Hill.
Betz, S. F., & Pielak, G. J. (1992) *Biochemistry 31*, 12337−12344.
Bowler, B. E., May, K., Zaragoza, T., York, P., Dong, A., & Caughey, W. S. (1993) *Biochemistry 32*, 183−190.
Bowler, B. E., Dong, A., & Caughey, W. S. (1994) *Biochemistry 33*, 2402−2408.
Brahms, S., & Brahms, J. (1980) *J. Mol. Biol. 138*, 149−178.
Brems, D. N., & Stellwagen, E. (1983) *J. Biol. Chem. 258*, 3655−3660.
Cohen, D. S., & Pielak, G. J. (1995) *J. Am. Chem. Soc. 117*, 1675−1677.
Cutler, R. L., Pielak, G. J., Mauk, A. G., & Smith, M. (1987) *Protein Eng. 1*, 95−99.
Das, G., Hickey, D. R., McLendon, D., McLendon, G., & Sherman, F. (1989) *Proc. Natl. Acad. Sci. U.S.A. 86*, 496−499.
Elöve, G. A., Bhuyan, A. K., & Roder, H. (1994) *Biochemistry 33*, 6925−6935.
Fersht, A. R., Matouschek, A., & Serrano, L. (1992) *J. Mol. Biol. 224*, 771−782.
Gao, Y., Boyd, J., Pielak, G. J., & Williams, R. J. P. (1991) *Biochemistry 30*, 1928−1934.
Gutte, B., & Merrifield, R. B. (1969) *J. Am. Chem. Soc. 91*, 501−502.
Hickey, D. R., Berghuis, A. M., Lafond, G., Jaeger, J. A., Cardillo, T. S., McLendon, D., Das, G., Sherman, F., Brayer, G. D., & McLendon, G. (1991) *J. Biol. Chem. 266*, 11686−11694.
Hilgen-Willis, S. (1993) Doctoral Dissertation, University of North Carolina at Chapel Hill.
Hilgen-Willis, S., Bowden, E. F., & Pielak, G. J. (1993) *J. Inorg. Biochem. 51*, 649−653.
Ikai, A., Fish, W. W., & Tanford, C. (1973) *J. Mol. Biol. 73*, 165−184.
IUPAC−IUB Joint Commission on Biochemical Nomenclature (1983) *J. Biol. Chem. 260*, 14−22.
Jackson, S. E., & Fersht, A. R. (1991) *Biochemistry 30*, 10436−10443.
Kiefhaber, T., Labhardt, A. M., & Baldwin, R. L. (1995) *Nature 375*, 513−515.
Komar-Panicucci, S., Weis, D., Bakker, G., Qiao, T., Sherman, F., & McLendon, G. (1994) *Biochemistry 33*, 10556−10560.
Koshy, T. I., Luntz, T. L., Plotkin, B., Schejter, A., & Margoliash, E. (1994) *Biochem. J. 299*, 347−350.
Levinthal, C. (1968) *J. Chim. Phys. Phys.-Chim. Biol. 65*, 44−45.
Linske-O'Connell, L. I., Sherman, F., & McLendon, G. (1995) *Biochemistry 34*, 7103−7112.
Louie, G. V., & Brayer, G. D. (1990) *J. Mol. Biol. 214*, 527−555.
Margoliash, E., & Frohwirt, N. (1959) *Biochem. J. 71*, 570−572.
Matouschek, A., & Fersht, A. R. (1993) *Proc. Natl. Acad. Sci. U.S.A. 90*, 7814−7818.
Matouschek, A., Kellis, J. T., Jr., Serrano, L., & Fersht, A. R. (1989) *Nature 340*, 122−126.
Matouschek, A., Kellis, J. T., Jr., Serrano, L., Bycroft, M., & Fersht, A. R. (1990) *Nature 346*, 440−445.
Matouschek, A., Otzen, D. E., Itzhaki, L. S., Jackson, A. R., & Fersht, A. R. (1995) *Biochemistry 34*, 13656−13662.
Milla, M. E., Brown, B. M., Waldburger, C. D., & Sauer, R. T. (1995) *Biochemistry 34*, 13914−13919.
Moore, G. R., & Pettigrew, G. W. (1990) *Cytochromes c: Biological Aspects*, Springer-Verlag, Berlin, Germany.
Murphy, K. P., Bhakuni, V., Xie, D., & Freire, E. (1992) *J. Mol. Biol. 227*, 293−306.
Muthukrishnan, K., & Nall, B. T. (1991) *Biochemistry 30*, 4706−4710.
Myers, J. K., Pace, C. N., & Scholtz, J. M. (1995) *Protein Sci. 4*, 2138−2148.
Nall, B. T. (1983) *Biochemistry 22*, 1423−1429.
Nall, B. T., & Landers, T. A. (1981) *Biochemistry 20*, 5403−5411.
Osterhout, J. J., Jr., & Nall, B. T. (1985) *Biochemistry 24*, 7999−8005.
Pace, C. N., Shirley, B. A., & Thomson, J. A. (1990) in *Protein Structure: A Practical Approach* (Creighton, T. E., Ed.) pp 311−330, IRL Press, Oxford, England.
Parker, M. J., Spencer, J., & Clarke, A. R. (1995) *J. Mol. Biol. 253*, 771−786.
Pielak, G. J., Oikawa, K., Mauk, A. G., Smith, M., & Kay, C. M. (1986) *J. Am. Chem. Soc. 108*, 2724−2727.
Ramdas, L., & Nall, B. T. (1986) *Biochemistry 25*, 6959−6964.
Ridge, J. A., Baldwin, R. L., & Labhardt, A. M. (1981) *Biochemistry 20*, 1622−1630.
Santoro, M. M., & Bolen, D. W. (1988) *Biochemistry 27*, 8063−8068.
Schellman, J. A. (1978) *Biopolymers 17*, 1305−1322.
Shortle, D., & Lin, B. (1985) *Genetics 110*, 539−555.
Shortle, D., & Meeker, A. K. (1986) *Proteins 1*, 81−89.
Spolar, R. S., Livingstone, J. R., & Record, M. T., Jr. (1992) *Biochemistry 31*, 3947−3955.
Tanford, C. (1970) *Adv. Protein Chem. 24*, 1−95.
Veeraraghavan, S., & Nall, B. T. (1994) *Biochemistry*, *33*, 687−692.
Willie, A., McLean, M., Liu, R.-Q., Hilgen-Willis, S., Saunders, A. J., Pielak, G. J., Sligar, S. G., Durham, B., & Millet, F. (1993) *Biochemistry*, *32*, 7519−7525.
Willis, S. H., Doyle, D. F., Auld, D. S., Betz, S. F., Fredericks, Z. L., Fencl, J. B., Bowden, E. F., & Pielak, G. J. (1993) *Protein Eng. 6* (Supple.), 25.
Weissman, J. S. (1995) *Chem. Biol. 2*, 255−260.
Wood, L. C., White, T. B., Ramdas, L., & Nall, B. T. (1988) *Biochemistry 27*, 8562−8568.

BI960409U